Scientific paper

Electropolymerized Polyaniline on Electrospun Silica Nanofibers to Prepare an SPME Fiber for the Sampling of Linear Alkylbenzenes

Kolsoum Dalvand[1], Marzieh Rashidipour[2,3,*], Alireza Ghiasvand[1]

[1] *Department of Chemistry, Lorestan University, Khoramabad, Iran*

[2] *Environmental Health Research Center, Lorestan University of Medical Sciences, Khorramabad, Iran*

[3] *Razi Herbal Medicines Research Center, Lorestan University of Medical Sciences, Khorramabad, Iran.*

** Corresponding author: E-mail: M_rashidi80@yahoo.com*
Tel/fax: +98 66 33120612, +98 66-33204007

Received: 06-14-2024

Abstract

An organic–inorganic polyaniline–silica (PANI/SiO_2) nanocomposite was synthesized through a combination of electrospinning and *in-situ* polymerization. This synthetic strategy effectively minimized PANI aggregation during polymerization, resulting in a higher yield and improved structural uniformity. Taking advantage of these enhanced properties, the nanocomposite was electrodeposited onto a stainless-steel wire and employed as an efficient sorbent for the extraction of linear alkylbenzenes (LABs) via headspace solid-phase microextraction (HS-SPME), followed by analysis using gas chromatography coupled with flame ionization detection (GC-FID). The structure and morphology of the synthesized sorbent were characterized using scanning electron microscopy (SEM) and Fourier-transform infrared spectroscopy (FT-IR) techniques. Response surface methodology (RSM) involving central composite design (CCD) was employed to evaluate the important experimental variables. Under the optimal conditions, linear dynamic ranges (LDRs) were in the range of 0.05–12 ng mL^{-1} for Φ-C11 (undecylbenzene) and Φ-C13 (tridecylbenzene), 0.02–12 ng mL^{-1} for Φ-C12 (dodecylbenzene) and Φ-C14 (tetradecylbenzene) with regression coefficient greater than 0.99. The limits of detection (LODs) were found to be 0.007–0.015 ng mL^{-1}. The developed HS-SPME-GC-FID method was successfully applied for extraction and determination of LABs in water and wastewater samples.

Keywords: Electrospinning; Polyvinyl alcohol; Silica nanofibers; Linear alkylbenzenes, Central composite design

1. Introduction

In 1990, Pawliszyn developed solid phase microextraction (SPME), a pre-treatment technique that combines sampling, extraction, analyte purification, and isolation from sample matrices in a single step.[1–3] His strategy is utilized in different analytical fields such as biological analysis,[4] food safety,[5–6] environmental monitoring,[7–8] and drug testing.[9] SPME technology is based on the partition equilibrium of analytes between the extraction phase and the sample matrix.[10–11] By changing the physical and chemical properties of the coating, higher efficiency and effectiveness can be achieved. Methods such as physical adhesion, immersion coating, electrophoretic deposition (EPD), chemical bonding, electrospinning method, physical vapor deposition (PVD),[12–13] among others, have been used for the preparation of SPME fibers.[11] Among these, electrophoretic deposition has been widely used due to advantages such as uniformity of deposits, simplicity, low-cost, and the ability to control the deposit thickness. EPD is usually employed in the processing of composite materials.[14–15] Polyaniline (PANI) is used as one of the conducting polymers in solid-phase microextraction techniques. In addition to environmental stability, high thermal and high sorption capability, it is conductive and can be deposited on different conductive substrates using EPD methods.[16–17] In the recent years, silica has emerged as a promising candidate for SPME methods due to its easy and low-cost preparation, biocompatibility, high specific surface area and as an abundant natural substance that can be easily prepared and manipulated to obtain more useful forms with high thermal and mechanical strength.[11,18] On

the other hand, polyaniline coated onto silica has attracted a lot of attention in separation techniques due to its special physical and chemical properties.[18]

Linear alkylbenzenes (LABs) are a group of organic compounds with the general formula $C_6H_5C_nH_{2n+1}$. LABs due to having side chains ranging C_{10} to C_{14} are routinely used in the manufacture of synthetic anionic surfactants known as alkylbenzene sulfonates (ABS). Usually, n ranges from 10 to 16, although generally supplied as a tighter cut, such as C_{12}–C_{15}, C_{12}–C_{13}, and C_{10}–C_{13}, for detergent use.[19–20] Although LABs are a potential chemical marker for the detection of domestic wastewater, they have been less studied due to analytical problems and limitations in their determination in aquatic environments.[21] In these studies, LABs were determined in marine sediments and wastewaters using gas chromatography-flame ionization detection (GC-FID) and gas chromatography-mass spectrometry (GC-MS) techniques. For this purpose, samples were preconcentrated by solid phase extraction (SPE), liquid-liquid extraction, thin layer chromatography and Soxhlet extraction methods before the analysis.[22–24]

In this study, polyaniline-coated silica nanofibers ($PANI/SiO_2$) were synthesized via a combined electrospinning and *in-situ* polymerization approach. Silica nanofibers were first prepared through electrospinning and subsequently employed as a structural template for the polymerization of aniline monomers. This integrated method enabled a uniform distribution of PANI nanoparticles over the SiO_2 nanofiber surface, effectively minimizing aggregation. The resulting composite was applied as a sorbent for the headspace extraction of linear alkylbenzenes (LABs) from wastewater samples using a fiber microextraction technique followed by gas chromatography with flame ionization detection (GC-FID). Experimental conditions were optimized using response surface methodology (RSM) based on a central composite design (CCD).

2. Experimental

2. 1. Materials

Undecylbenzene (ϕ-C11), dodecylbenzene (ϕ-C12), tridecylbenzene (ϕ-C13), and tetradecylbenzene (ϕ-C14), all with purities > 99%, were purchased from Sigma-Aldrich (Darmstadt, Germany). A mixed standard stock solution (1000 μg mL^{-1}) was prepared by dissolving appropriate amounts of the LABs in acetonitrile. The working standard solutions were prepared from the stocks weekly. All stock and working solutions were kept at 4 °C. Analytical reagent grade ammonium persulfate (99.5%), tetraethoxysilane (TEOS, 98%), hydrochloric acid (37%), phosphoric acid (85%), nitric acid (70%), and sulfuric acid (98%) were purchased from Merck (Darmstadt, Germany), as well as chromatography-grade ethanol and methanol. Aniline (99.5%) was purchased from Merck and the required amount of aniline was redistilled prior to each use and stored in a dark bottle in a refrigerator. Polyvinyl alcohol (PVA, for synthesis, partially hydrolyzed, M_w~70000) was purchased from Sigma-Aldrich (Darmstadt, Germany).

2. 2. Instrumentation

In this research, analysis of the LABs compounds was accomplished by gas chromatography-flame ionization detection (GC-2010 Plus-AF), which was designed and manufactured by Shimadzu (Kyoto, Japan). GC solution software (version 2.4.1) was used for operation of the GC system. Chromatographic separations and determinations were performed using a BPX-5 fused silica capillary column with 0.25 μm film thickness, 30 m length, and 0.25 mm internal diameter. Oven temperature was programmed from initial 180 °C, held for 1 min, to 200 °C at a rate of 2 °C min^{-1}, and finally raised to 280 °C with a heating rate of 4 °C min^{-1} and kept constant for 4 min. The total run time was 35 min.

The injector and detector were set at 280 and 300 °C, respectively. All SPME injections were done in split mode (ratio 1:10). Ultrapure nitrogen (>99.99%) was used as carrier gas at a flow rate of 1 mL min^{-1}. Flow-rates of hydrogen, zero-air, and nitrogen (make-up gas) were set at 30, 300, and 30 mL min^{-1}, respectively. Minitab® 17 software was applied for the design of the experiments. An Eppendorf micropipette (Eppendorf, Hamburg, Germany) and 10, 50, 100, and 500 μL SGE microsyringe (SGE, Sydney, Australia) were used to measure and deliver accurate volumes of solvents and solutions. A Shimadzu Fourier transform infrared spectra were recorded using a FT-IR 8400 spectrometers in the transmittance mode. The morphology of the $PANI/SiO_2$ nanocomposite was observed with CM120 Vega field-emission scanning electron microscope (Tescan, Brno, Czech Republic). Thermogravimetric analysis (TGA) data were recorded on Q-600 TGA system (TA Instruments, America). The electrospinning experiments were performed using a Full Option Lab2 ESI-II system (Nanoazma Co., Tehran, Iran).

2. 3. Preparation of the $PANI/SiO_2$ Coated Fiber

Silica nanofibers were synthesized via hydrolysis of tetraethyl orthosilicate (TEOS) following a previously reported method. Briefly, 4.00 g of TEOS was mixed with 3.75 mL of distilled water and 1.25 mL of ethanol under stirring. Phosphoric acid (H_3PO_4, 0.10 mL) was then added dropwise, and the mixture was stirred for 5 h. Subsequently, 15.0 g of 9% *w/w* polyvinyl alcohol (PVA) solution was incorporated and stirred for an additional 8 h to obtain a spinnable sol. The sol was electrospun at 13 kV with a flow rate of 0.5 mL/min and a tip-to-collector distance of 15 cm. The collected nanofibers were dried at 60 °C for 12 h and calcined at 550 °C for 8 h to remove the PVA tem-

plate.[25] To fabricate a robust and durable PANI/SiO_2 coated SPME fiber, the stainless-steel wire was cut into pieces of 3 cm and first washed with methanol and water. Then, the tips of the stainless-steel fibers were dipped (1 cm) into a stirring nitric acid solution (1 M) for 40 s, to generate a rough surface.

The SiO_2 nanofibrous, weighing 0.08 g, was dispersed in 6 mL of 0.5 M sulfuric acid and 0.2 M aniline solution for 30 min to obtain an electrolyte for the electropolymerization. The stainless-steel fiber was connected to the anode and a normal stainless-steel wire was connected to the cathode with 1 cm distance from the anode. Afterwards, a 1.5 V constant DC voltage was applied to the system for 20 min. Finally, the PANI/SiO_2 fiber was removed from the electrochemical cell and washed with water and dried. Before the first use the fiber was preconditioned under nitrogen atmosphere for 30 min at 280 °C by placing into a GC injection port.

2. 4. Sampling and Quantification of LAB Using the PANI/SiO_2 Fiber

The PANI/SiO_2 coated fiber was used for the extractions of LABs in wastewater. For this purpose, 10 mL sample solution containing 0.5 μg mL^{-1} of LABs and 8% (*w/v*) sodium chloride was placed into a 10 mL SPME vial inside a water bath at 62 °C with stirring at 600 rpm and the SPME fiber was passed through the vial septum and placed in the headspace of the sample. After 15 min, the fiber tool was removed and inserted at temperature of 280 °C for 2 min into the GC–FID injection port for the thermal desorption and analysis.

3. Results and Discussion

3. 1. Characterization of the PANI/SiO_2 SPME Sorbent

To characterize the functional groups of the prepared sorbent, FT-IR spectroscopy was employed. The FT-IR spectrum of silica showed three main characteristic bands at 1112.85, 808.12, and 470 cm^{-1}, corresponding to the asymmetric stretching, symmetric stretching, and bending vibrations of Si–O–Si bonds, respectively, as shown in Fig. 1a and previously reported in the literature.[26] Fig. 1 presents the FTIR spectra of SiO_2 (a), the PANI/SiO_2 composite (b), and pure PANI (c). In spectrum (c), characteristic bands of PANI are observed at 1583 and 1508 cm^{-1}, corresponding to the stretching vibrations of the C=N and C=C bonds, respectively. Additional absorption bands at 1298 cm^{-1} and 1149 cm^{-1} are attributed to C–N and N–H stretching vibrations within the benzenoid rings. A broad band around 3265 cm^{-1} is also detected, which is associated with the N–H stretching vibration of aromatic amine groups. Similar features appear in the spectrum of the PANI/SiO_2 composite (b), with bands at 1583.45 and 1544.23 cm^{-1}, confirming the successful incorporation of PANI into the composite matrix.[25, 27–29]

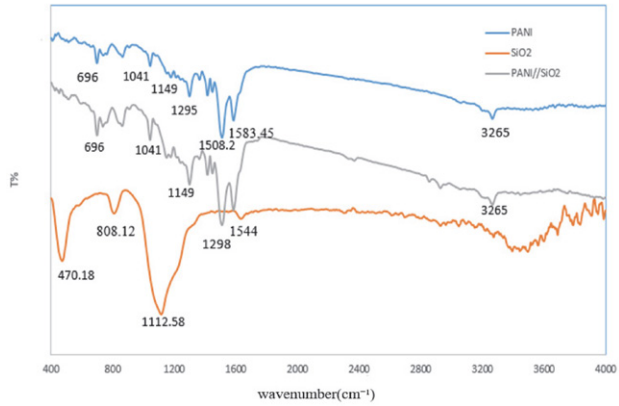

Fig. 1. The FT-IR spectra of (a) SiO_2, (b) PANI/SiO_2, c) PANI.

The structure and morphology of the PANI/SiO_2 nanocomposite were examined using a SEM instrument. Fig. 2 shows the SEM images of SiO_2, PANI, and PANI/SiO_2 nanofibers. The smooth surface and uniform morphology of SiO_2 nanofibers are evident from Fig. 2(a). Fig. 2(b) illustrates the morphology of pure PANI, where polyaniline particles tend to aggregate during the polymerization process, thereby reducing sorption capacity and porosity. The synthesis of silica nanofibers by electrospinning provides a template to prevent this aggregation.[30] This is evident from Fig. 2(b) and 2(c), where the silica nanofibers clearly form a network structure, and the PANI particles are deposited on them. This observation supports the claim that the silica nanofibers act as a template to prevent aggregation. As shown in Fig. 2(c), PANI nanoparticles are uniformly coated on the surface of the silica nanofibers, enhancing adsorptivity, flexibility, and permeability. Additionally, Fig. 2(d) presents a higher magnification image of the PANI/SiO_2 composite, confirming the homogeneous distribution and strong adhesion of PANI particles on the SiO_2 nanofiber surface. To further substantiate this observation, additional SEM images at higher magnifications have been included (Fig.2e and 2f). These images clearly demonstrate the uniform and continuous coating of PANI nanoparticles on the silica nanofibers. The nanoparticles are homogeneously distributed without significant aggregation or gaps, indicating a consistent morphology and coverage. This confirms the effectiveness of the synthesis and coating process, which is expected to improve the functional properties of the nanocomposite.[25,29] The EDX spectrum recording was also carried out on the sorbent (Fig. 3). The elemental mass ratios of silicon, oxygen, carbon, and nitrogen were 6.4, 30.5, 46.6, and 15.9%, respectively. These

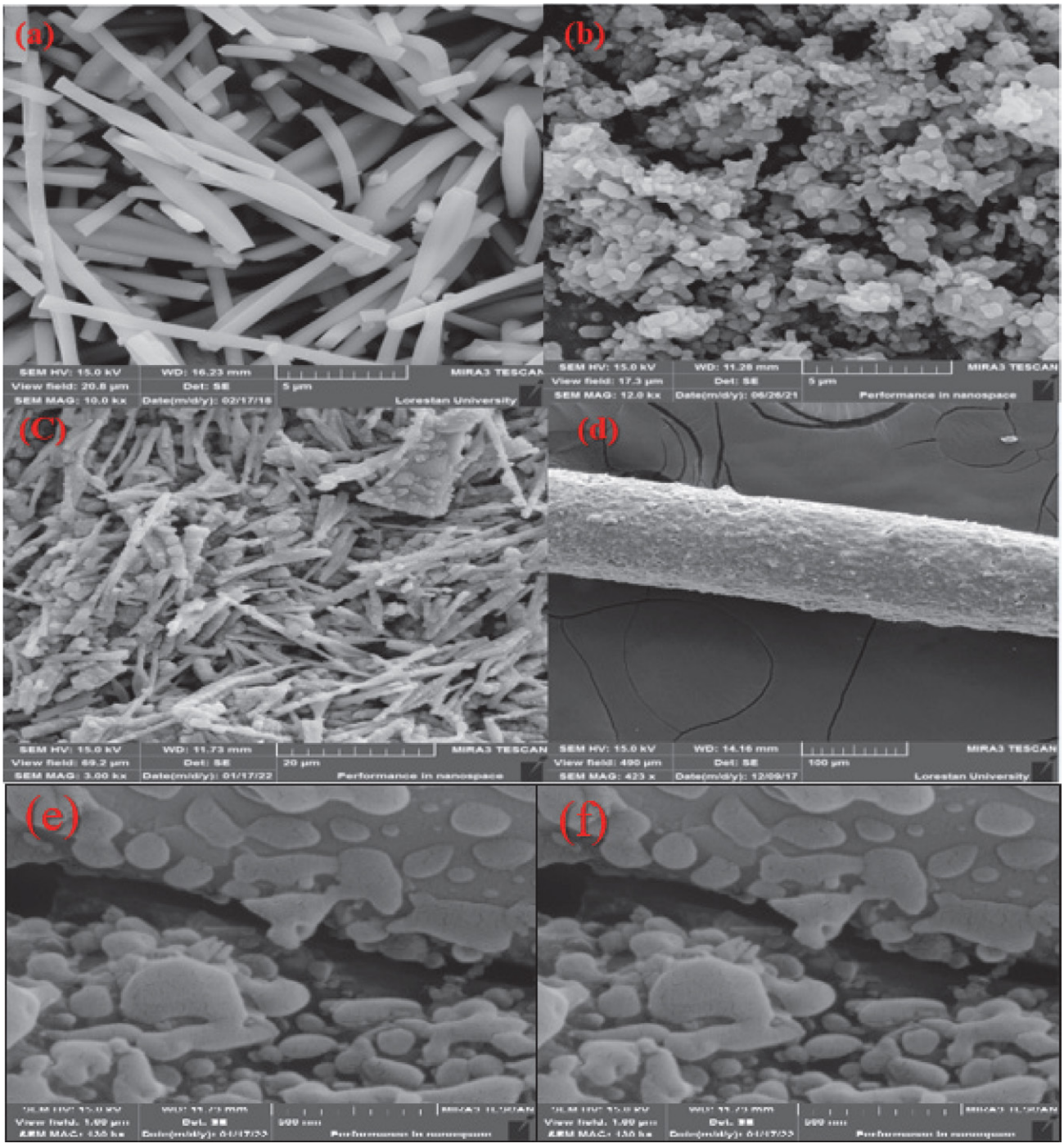

Fig. 2. SEM micrographs of silica nanofibers (a), PANI (b), PANI /Silica nanofibers(c), surface of the fiber coated by PANI/SiO_2 film (d), Polyaniline at different magnifications (e) and (f).

results show a good accordance with the PANI particles, synthesized on the surface of silica nanofibers.

Thermogravimetric analysis (TGA) was conducted to assess the thermal stability of the synthesized composite, given its intended exposure to the elevated temperatures of the gas chromatography (GC) injection port during SPME-GC analysis. This evaluation ensures the material's suitability for high-temperature applications. The TGA curves of PANI/SiO_2 nanofibers are presented in Fig. 4. TGA has been performed in the temperature range of 30–800 °C with a rate of 10 °C per min under air atmosphere. As Fig. 4 shows, the temperature of thermal decomposition of PANI/SiO_2 nanofibers is about 300 °C. The initial weight loss observed in the thermogravimetric analysis (TGA), typically occurring below 150 °C, is primarily attributed to the release of physically adsorbed

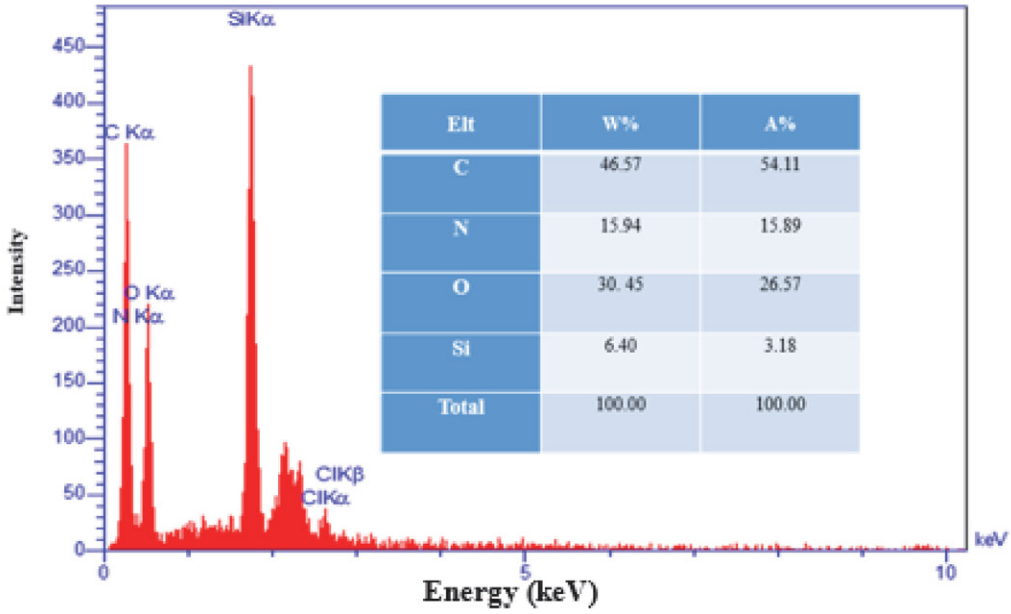

Fig. 3. The EDX microanalysis results for the PANI/Silica nanofibers.

water molecules and the evaporation of residual unreacted monomers. These species are retained within the material through weak interactions such as hydrogen bonding or van der Waals forces and are not chemically bonded to the main structure. Consequently, the observed mass loss at this stage corresponds to the removal of physically bound volatile components rather than any chemical degradation. Such behavior is commonly observed in polymeric or hybrid materials that may retain moisture or unreacted monomers due to synthesis or storage conditions.[31–33]

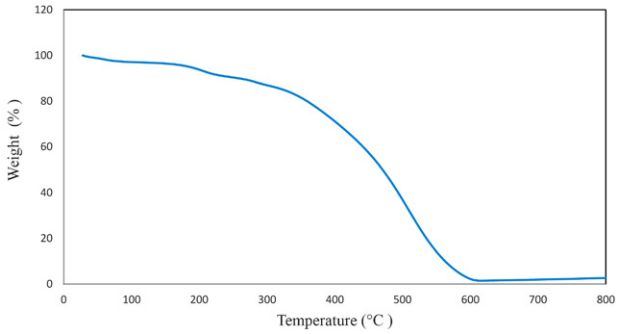

Fig. 4. TGA of PANI/Silica nanofibers.

3. 2. Optimization of the Extraction Conditions Using CCD

To achieve the maximum extraction efficiency, high pre-concentration, and accurate results in the shortest possible time, the main parameters including extraction time, ionic strength, extraction temperature, stirring rate, and desorption conditions were optimized. Since the adsorption characteristics of the PANI/SiO_2 fiber were initially unknown, desorption time and temperature were optimized using a one-variable-at-a-time approach to ensure complete desorption of the adsorbed analytes. The optimization range was selected based on previous experience with various sorbents, including PANI/SiO_2. Lower temperatures and shorter desorption times are insufficient for complete analyte desorption, whereas higher temperatures and prolonged durations may lead to sorbent degradation. Accordingly, desorption time and temperature were varied within the ranges of 1–5 min and 230–280 °C, respectively. The results demonstrated that the highest extraction efficiency for the proposed nanocomposite fiber was obtained at a desorption time of 1 min and a temperature of 280 °C.

Then, the CCD design was employed to determine the optimal extraction conditions through RSM. Multivariate optimization has important advantages over one-at-a-time, such as reducing the number of experiments, studying the interaction between variables, which leads to faster and more efficient optimization. Central composite design (CCD) is a member of the RSM, which is a way to identify optimal experimental conditions with a reasonable number of runs. In general, the number of experimental runs is given by $\mathbf{2^k+2}\,\boldsymbol{k}\mathbf{+}\boldsymbol{C_p}$ (where k and C_p are the number of factors and the number of central points, respectively). Statistical software of Minitab 17 (State College, PA, USA) was employed to generate the design matrix and to assess the results.[33–34] In this study, four extraction variables, including extraction time, sample temperature, ionic strength, and stirring rate were considered for the RSM-CCD optimization. For each variable, five levels (0, –α, +α, –2α, and +2α) were assigned as the central points, low axial runs, high axial runs, the experimental variables, and five levels for the

CCD optimization are shown in Table 1. The design matrix and the responses (peak area) are listed in Table 2. Analysis of variance (ANOVA) was applied to ensure the accuracy of the proposed RSM model.[34–35] The obtained results are presented in Table 3. Based on the results, the p-values of the independent factors were <0.05, while the p-values of the Lack-of-Fit were higher than 0.05, confirming that all variables were statistically significant with 95% confidence level. According to the ANOVA results, a second-order polynomial equation was fitted using the following equation:

$$= 74075 + 1844\ T + 8065\ t - 33255\ IS - 280.6\ SR - 23.09\ T^2 - 92.78\ t^2 + 2238\ IS^2 + 0.2496\ SR^2 - 36.11\ T \times t + 278.2\ T \times IS - 0.086\ T \times SR - 150.1\ t \times IS - 0.990\ t \times SR + 8.02\ IS \times SR$$

The value of determination regression coefficients (R^2 = 0.9935) also indicated that the polynomial model fits well. Besides, predicted-R^2 and adjusted-R^2 were 0.9585 and 0.9866, respectively, which shows a desirable value for the statistical model validation.

The 3D response surfaces were created to obtain the optimal values and interactive effects of the independent variables, as shown in Fig. 5 for Φ-C13. The optimal values for extraction temperature, extraction time, ionic strength, and stirring rate were determined to be 62 °C, 15 min, 8%, and 600 rpm, respectively. The interaction between the variables is shown using the charts of the interruption.

Fig. 6 presents the main and interaction effects of key parameters on Φ-C12 extraction. The main effects plot (Fig. 6a) indicates that extraction efficiency generally increases with higher temperatures, ionic strength, and stirring rates. However, extraction time shows an optimal point around 15 min. The interaction plot (Fig. 6b) reveals that temperature significantly influences the effect of extraction time; at lower temperatures (20–35 °C), extraction time has minimal impact, while at higher

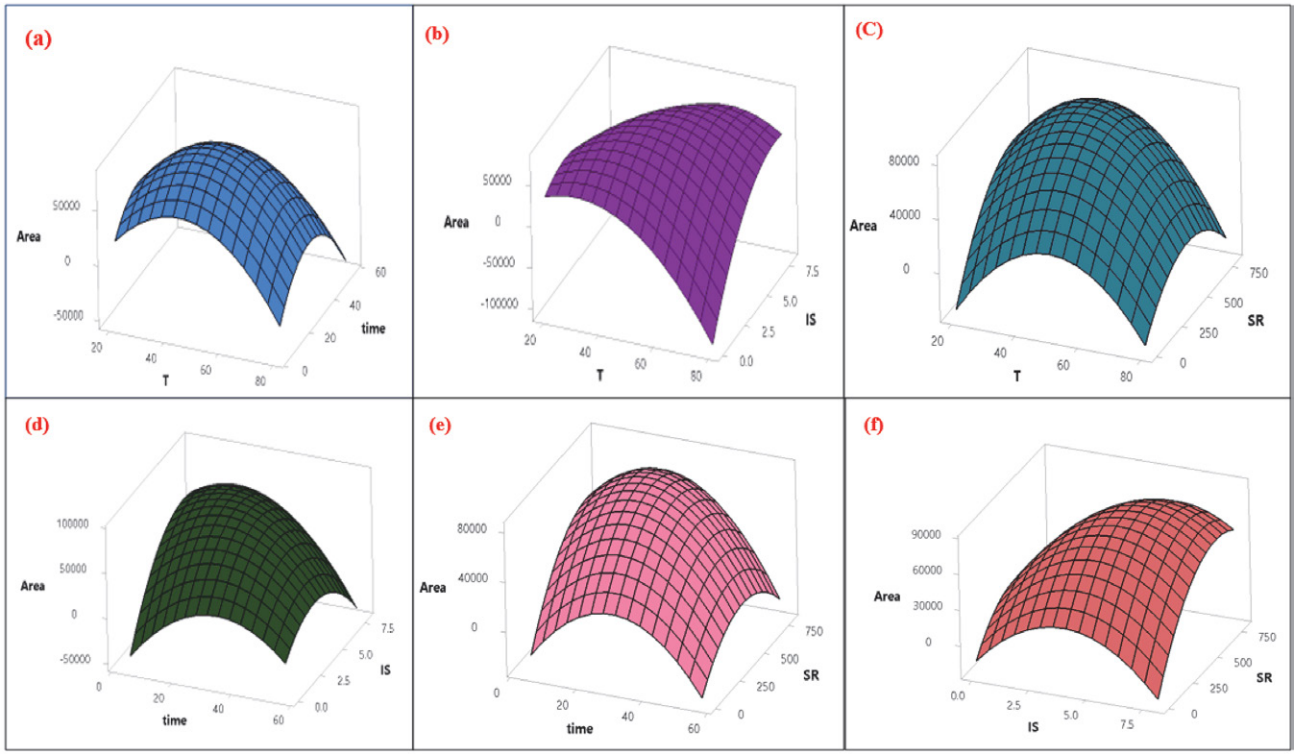

Fig. 5. Response surfaces for extraction temperature/extraction time (a), extraction temperature/ionic strength (b), extraction temperature/stirring rate (c), extraction time/ionic strength (d), extraction time/stirring rate (e), and ionic strength/stirring rate (f).

Table 1. Experimental factors and levels used in the CCD model.

Variable (Symbol, Unit)	Levels				
	Low axial (-2α)	Low factorial (–1)	Center point (0)	High factorial (+1)	High axial (+2α)
Sample temperature (*T*, °C)	20	35	50	65	80
Extraction time (*t*, min)	5	18	31	44	57
Ionic strength (IS, *w*/*v*%)	0	2	4	6	8
Stirring rate (SR, rpm)	0	200	400	600	800

Table 2. The CCD matrix and the obtained data at different levels of the experimental factors.

RunOrder	*T*	*t*	IS	SR	Φ-C11	Φ-C12	Φ-C13	Φ-C14
1	50	31	4	400	79398	69865	70572	45990
2	50	31	4	800	85087	77143	60665	5955
3	50	31	8	400	109937	70790	45432	52234
4	20	31	4	400	80841	3036	28173	8394
5	50	31	4	0	160257	31989	12061	38831
6	50	5	4	400	30665	32696	34758	7211
7	50	31	0	400	127162	23890	9266	20576
8	80	31	4	400	43069	69174	4442	41634
9	50	57	4	400	9373	10056	6930	33742
10	50	31	4	400	84056	68756	80125	44423
11	35	44	2	600	79892	16056	43354	40214
12	50	31	4	400	79292	70056	77908	59662
13	65	18	2	600	60392	61844	12047	24824
14	65	44	2	200	78756	48682	12695	55905
15	65	18	6	600	79057	152521	80362	70036
16	65	18	6	200	97702	36517	55546	74432
17	35	44	6	600	49513	20493	35915	30056
18	35	44	2	200	120768	48120	48901	70307
19	35	18	6	200	80189	28957	43758	40602
20	50	31	4	400	75500	70073	80065	59964
21	65	18	2	200	92056	13994	7872	32669
22	65	44	2	600	34954	45165	8126	40569
23	35	18	2	600	75188	50612	72794	12152
24	35	18	6	600	60420	80696	73946	26481
25	65	44	6	600	35193	110036	38258	37336
26	50	31	4	400	79809	75056	79656	57955
27	50	31	4	400	75418	66557	85015	59111
28	35	18	2	200	110425	44925	43669	13745
29	35	44	6	200	77456	5243	2050	50189
30	65	44	6	200	69056	51745	30056	65384

Table 3. ANOVA for the suggested CCD model.

Term	Φ-C11			Φ-C12			Φ-C13			Φ-C14		
	Coef	T	P	Coef	T	P	Coef	T	P	Coef	T	P
T	−7593	−10.49	0.000	14528	12.02	0.008	−6954	−5.36	0.000	7662	12.01	0.000
t	−6351	−8.77	0.000	−7075	−5.71	0.005	−9429	−7.26	0.000	6170	9.67	0.000
IS	−5762	−7.96	0.000	10442	8.42	0.000	7615	5.87	0.000	6977	10.94	0.000
SR	−16756	−23.15	0.000	14565	11.75	0.003	9061	6.98	0.000	−7805	−12.24	0.000
T×T	−5195	−7.67	0.000	−6634	−5.72	0.000	−13501	−11.12	0.000	−4587	−7.69	0.000
t×t	−15679	−23.16	0.000	−10316	8.89	0.000	−12367	−10.18	0.000	−5721	9.59	0.000
IS×IS	8953	13.22	0.000	−3825	−3.30	0.005	−10741	−8.84	0.000	−1739	−2.91	0.011
SR×SR	9984	14.74	0.000	−2019	1.74	0.104	−8487	6.99	0.000	−5242	−8.79	0.000
T×t	−7041	−7.94	0.000	6627	4.36	0.001	2328	1.46	0.165	−6285	−8.04	0.000
T×IS	8347	9.41	0.000	12841	8.46	0.000	13533	8.51	0.000	55144	6.59	0.000
T×SR	−259	−0.29	0.774	11126	7.33	0.000	−3438	−2.16	0.048	645	0.83	0.423
t×IS	−3904	−4.40	0.001	−6114	4.03	0.001	−7752	−4.87	0.000	−9512	−12.18	0.000
t*SR	−2573	−2.90	0.012	−11457	−7.54	0.000	−3522	2.21	0.044	−4103	−5.25	0.000
IS*SR	3210	3.62	0.003	27916	9.19	0.000	4618	2.90	0.012	−739	−0.95	0.360

temperatures (50–80 °C), efficiency peaks sharply around 15 min. Similarly, at high ionic strength (IS), different levels of stirring rate (SR) did not contribute to extraction, which at low IS, increasing SR increased extraction of Φ-C12. These findings suggest optimizing temperature and extraction time is crucial for maximizing Φ-C12 extraction efficiency.

Fig. 7 shows the normal probability plot for Φ-C13; it is clear that the distribution of residuals is normal, and the model satisfies the assumptions of the analysis of variance.

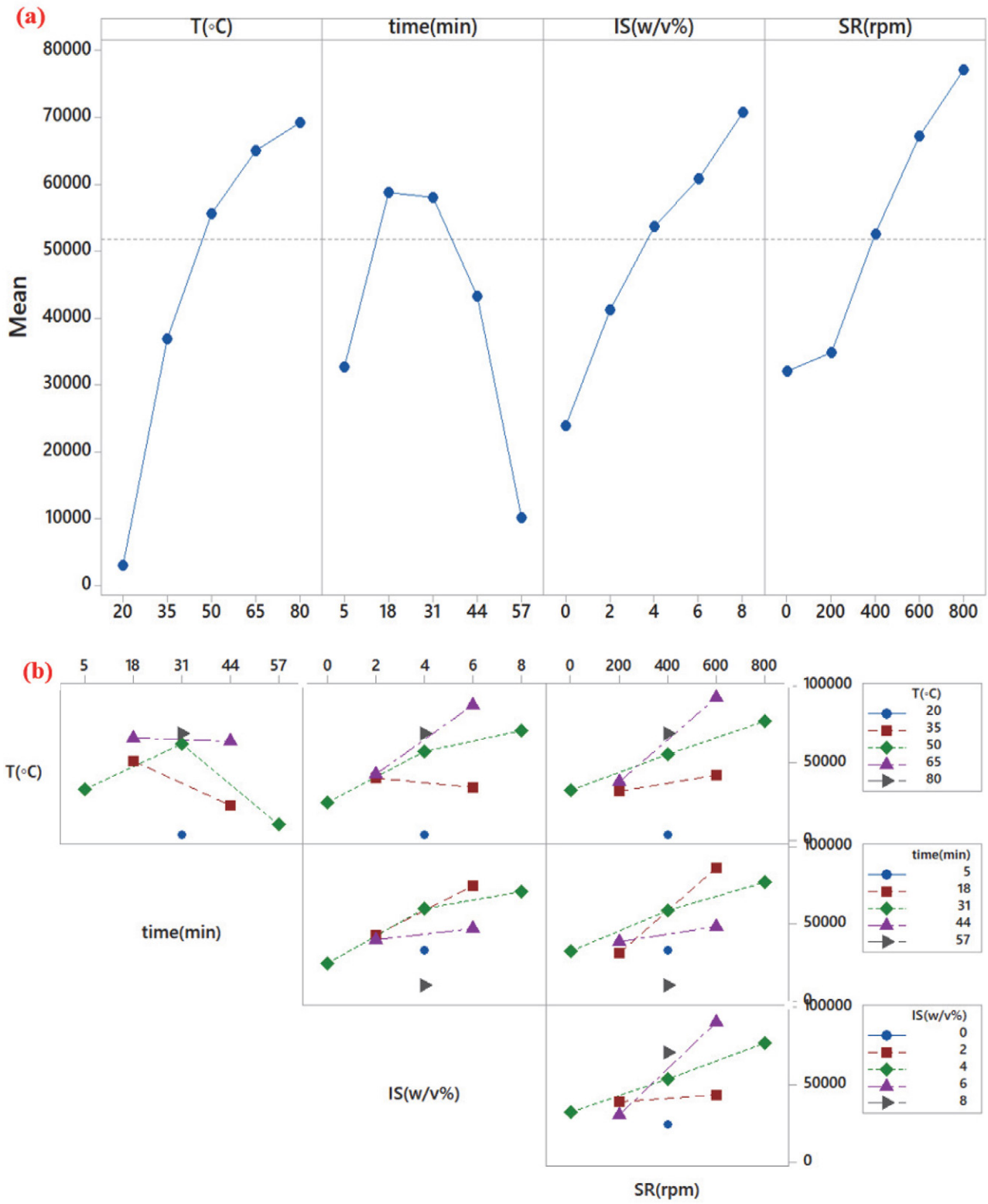

Fig. 6. The a) main effects and b) interaction plots for Φ-C12.

3. 3. Analytical Figures of Merit

Analytical figures of merit of the purpose method, involving linear dynamic ranges (LDRs) relative standard deviations (RSDs), and detection limits (LODs) for the determination of four LABs in aqueous samples were evaluated. The results are shown in Table 4. The calibration graphs were linear in the ranges of 0.05–12 ng mL^{-1} for Φ-C11 and Φ-C13 and 0.02–12 ng mL^{-1} for Φ-C12

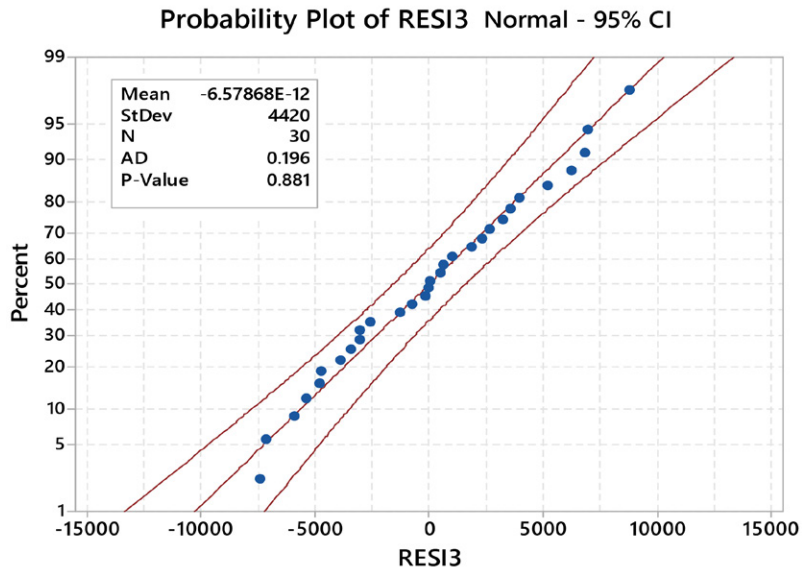

Fig. 7. The probability plot for Φ-C13.

and Φ-C14 with linear regression coefficients greater than 0.9947. The limits of the detection (LODs) and limits of quantitation (LOQs), defined as S/N = 3 and S/N = 10, respectively, the results of which are presented in Table 4.

The relative standard deviations (RSDs, $n = 6$) values for a single fiber (repeatability) were determined 4.8–7.3%. The inter-fiber RSDs (reproducibility) for three randomly selected fibers were in the range of 9.2–12.4%. For further evaluation of the reliability and applicability, the analytical performances of the developed method were compared with some similar previous studies,[36–38] reported on the separation and determination of LABs (Table 5). The results clearly showed that the proposed method has a wider LDRs and lower LODs compared to the mentioned meth-

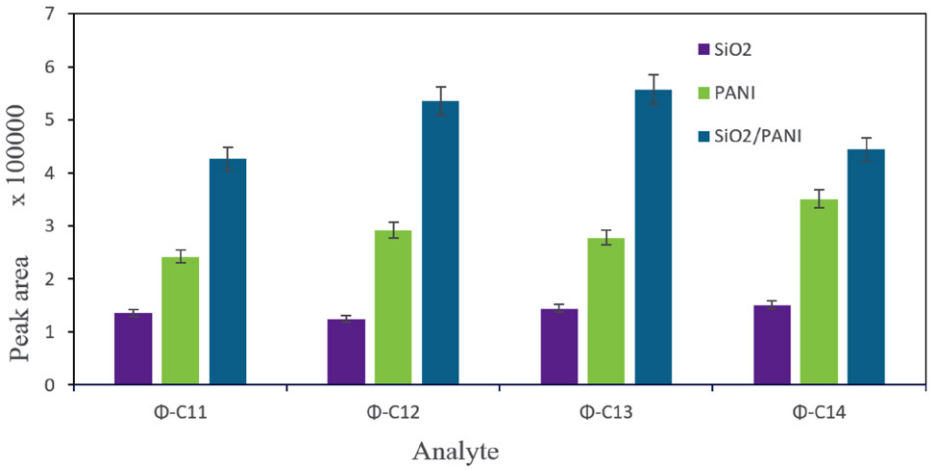

Fig. 8. Comparison of the trapping efficiency of LABs using fibers prepared by different sorbents.

Table 4. Analytical figures of merit for the analysis of LABs using the PANI/SiO_2 fiber nanosorbent.

Analytes	LDR (ng mL^{-1})	Equation	R^2	LOD (ng mL^{-1})	LOQ (ng mL^{-1})	RSD (%) Intra-fiber ($n = 6$)	Inter-fiber ($n = 3$)
Φ-C11	0.05–12	y = 8672x + 14527	0.995	0.015	0.05	6.9	9.2
Φ-C12	0.02–12	y = 6636x + 9597	0.996	0.007	0.02	4.8	10.2
Φ-C13	0.05–12	y = 5044x + 9775	0.996	0.015	0.05	5.6	11.2
Φ-C14	0.02–12	y = 3327x + 8989	0.996	0.007	0.02	7.3	12.4

Table 5. Comparison of the developed HS-SPME/GC procedure with some similar SPME methods reported for the analysis of LABs in wastewater samples.

Method	RSD (%)	LOD (ng mL^{-1})	LDR (ng mL^{-1})	Matrix	Ref.
In-tube SPME-HPLC-UV	1.6–12	0.02–0.1	0. 2–25	aqueous samples	[38]
INCAT SPME-GC-FID	5.3–16.9	0.5–1	0.01–10	wastewater	[37]
Ion pair-SPME-GC-MS	10–12	0.16–0.8	0.5–2.4	water	[36]
HS-SPME-GC-FID	4.8–12.4	0.007–0.015	0.02–12	wastewater	This work

ods. To evaluate the efficiency of PANI/SiO_2 fibers for extracting linear alkylbenzenes from aqueous samples under optimized conditions, fibers containing polyaniline, silica, and the PANI/SiO_2 composite were prepared, and their extraction efficiencies were compared (Fig. 8). The enhanced extraction efficiency of the PANI/SiO_2 composite fibers for linear alkylbenzenes (C11–C14) compared to individual polyaniline or silica fibers is due to the synergistic interaction between the sorbent materials and the analytes. Linear alkylbenzenes become less polar and more hydrophobic as the alkyl chain length increases. Silica's highly polar surface exhibits low affinity for these non-polar compounds, whereas polyaniline's moderate polarity and aromatic structure enable π–π interactions and hydrogen bonding with the analytes. Combining these materials in the composite fiber increases both the variety and strength of interactions, improving extraction performance. Additionally, the aqueous medium's pH can affect polyaniline's protonation state, further modulating its interaction with analytes.

3. 4. Real Samples and Apparent Recovery

To evaluate the reliability and applicability of the developed method, it was employed for the analysis of LABs in three real wastewaters and the apparent recovery was estimated. One sample (#1) was of a municipal wastewater (Khoramabad, Iran) and two samples (#2 and #3) were from the Khoram River passing through the city of Khoramabad. All samples were collected and stored according to a standard sampling method.[39] In order to estimate the apparent recovery, each real sample was first analyzed under optimized conditions to determine its initial analyte concentration (B). Then, a standard solution was added (spiked) to the same sample at three different concentration levels: one near the limit of quantification (LOQ), one at the middle level, and one at the highest concentration of the calibration range. The spiked samples were then reanalyzed. The results are presented in Table 6.

The apparent recovery (R) was calculated using the following equation:

$$R\% = \frac{(C - B)}{A} \times 100$$

where A is the added (spiked) concentration, B is the initial concentration of real sample, and C is the concentration of the fortified real sample.

This approach provides an estimate of the combined effects of extraction efficiency and matrix influence on the analyte quantification, although it does not isolate the matrix effect as defined by post-extraction spiking or slope comparison methods.[40] The results showed that the R% values were distributed over the range 90.0–120.0% and demonstrated that the influences on the recovery were not significant. A sample chromatogram of one of the real samples is depicted in Fig.9.

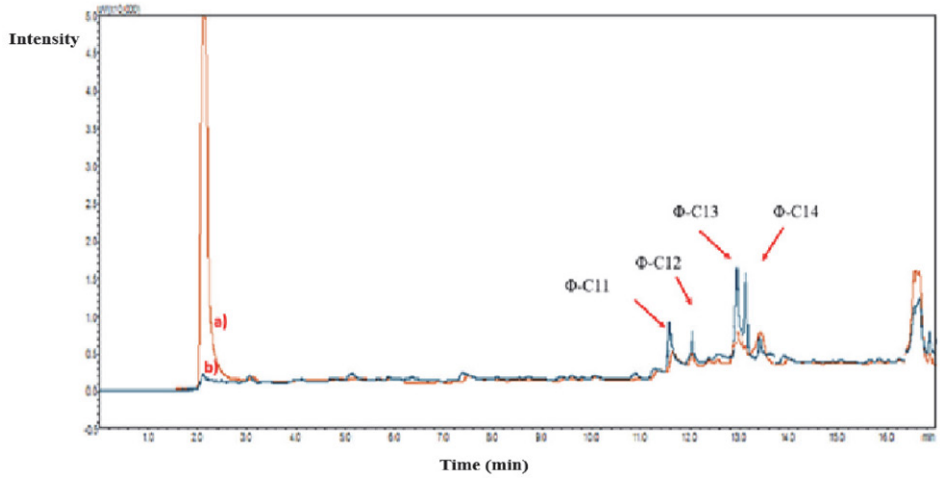

Fig. 9. GC-FID chromatograms of the LABs extracted from a real sample, before (a) and after spiking (b) with a mixed standard solution of the analytes.

Table 6. Recovery rates of LABs from samples spiked at three levels within the LDR.

Analyte	Added	Φ-C11		Φ-C12		Φ-C13		Φ-C14	
	(ng mL^{-1})	Determined	R%	Determined	R%	Determined	R%	Determined	R%
Wastewater	0	0.11 (3.11)[a]	–	0.12 (2.41)	–	0.08 (4.31)	–	0.05 (3.21)	–
	0.2	0.29 (1.90)	95.0	0.31 (2.50)	100.0	0.31 (3.10)	95.0	0.25 (2.30)	100.0
	6	5.78 (2.60)	94.7	5.61 (3.51)	92.2	6.01 (3.12)	98.8	5.81 (3.21)	95.7
	10	10.01 (2.51)	99.1	9. 61 (2.12)	94.4	9.90 (1.51)	98.1	10.01 (3.01)	99.6
River water #1	0	0.04 (3.11)	–	0.05 (3.61)	–	ND[b]	–	ND	–
	0.2	0.25 (2.51)	105.0	0.23 (2.42)	90.0	0.18 (2.71)	90.0	0.21 (2.90)	99.5
	6	6.01 (1.81)	99.5	6.01 (2.81)	99.3	5.90 (3.60)	98.0	5.50 (4.10)	90.2
	10	10.01 (2.31)	99.7	9.61 (3.82)	95.1	9.91 (4.61)	98.9	10.10 (3.21)	101.0
River water #2	0	0.03 (2.51)	–	0.01 (5.21)	–	0.01 (2.40)	–	0.02 (3.11)	–
	0.2	0.21 (4.11)	90.0	0.19 (3.12)	90.0	0.25 (3.50)	120.0	0.24 (2.10)	111.0
	6	6.1 (2.31)	100.8	6.01 (2.80)	100.0	6.10 (3.11)	101.2	6.07 (4.60)	100.8
	10	10.03 (3.10)	100.0	9. 61 (1.80)	95.5	9.81 (4.20)	97.8	10.10 (3.91)	101.0

[a] The numbers in parentheses refer to RSD% obtained by three replicated analyses. [b] Not detected

4. Conclusions

In this work, a PANI/SiO_2 nanofibrous sorbent was successfully fabricated via an integrated electropolymerization-electrospinning approach, yielding a stable and high surface-area material suitable for analytical applications. Coupling the sorbent with GC-FID enabled efficient headspace extraction and quantification of linear alkylbenzenes (LABs) in complex wastewater matrices. Method optimization through central composite design led to a significant enhancement in the analytical performance parameters, including extended linear dynamic ranges (LDRs), low limits of detection (LODs), and satisfactory precision (RSDs). Comparative evaluation against existing methodologies confirmed the superiority of the developed system in terms of sensitivity and reliability. These findings demonstrate the potential of the PANI/SiO_2 nanofiber as a versatile sorptive phase for environmental analysis. Future work will involve integration with GC–MS platforms to facilitate the trace-level determination of emerging organic pollutants in environmental samples.

Acknowledgments

The authors gratefully appreciate the support of the Environmental Health Research Center of Lorestan University of Medical Sciences (grant number: 2146; Ethical code: IR.LUMS.REC.1400.180).

5. References

1. Arthur, C. L.; Pawliszyn, J., *Anal. Chem.* **1990**, *62* (19), 2145–2148 **DOI:**10.1021/ac00218a019
2. Szultka-Młyńska, M.; Janiszewska, D.; Pomastowski, P.; Złoch, M.; Kupczyk, W.; Buszewski, B., *Molecules* **2021**, *26* (16), 5007. **DOI:**10.3390/molecules26165007
3. Zheng, J.; Huang, J.; Xu, F.; Ni, C.; Xie, X.; Zhu, F.; Wu, D.; Ouyang, G., *Nanoscale* **2018**, *10* (12), 5725–5730 **DOI:**10.1039/C7NR08010G
4. Varona, M.; Ding, X.; Clark, K. D.; Anderson, J. L., *Anal. Chem.* **2018**, *90* (11), 6922–6928. **DOI:**10.1021/acs.analchem.8b01160
5. Lv, F.; Gan, N.; Cao, Y.; Zhou, Y.; Zuo, R.; Dong, Y., *J. Chromatogr. A* **2017**, *1525*, 42–50. **DOI:**10.1016/j.chroma.2017.10.026
6. Nasrollahpour, A.; Moradi, S. E., *J. AOAC Int.* **2019**, *101* (5), 1639–1646. **DOI:**10.5740/jaoacint.17-0374
7. Mohammadi Toudeshki, R.; Dadfarnia, S.; Haji Shabani, A. M., *New J. Chem.* **2018**, *42* (13), 10751–10760 **DOI:**10.1039/C8NJ01670D
8. Toudeshki, R. M.; Dadfarnia, S.; Shabani, A. M. H., *New J. Chem.* **2018**, *42* (13), 10751–10760 **DOI:**10.1039/C8NJ01670D
9. Wang, Y.; Jie, Y.; Hu, Q.; Yang, Y.; Ye, Y.; Zou, S.; Xu, J.; Ouyang, G., *J. Chromatogr. A* **2020**, *1623*, 461171 **DOI:**10.1016/j.chroma.2020.461171
10. Feng, J.; Feng, J.; Ji, X.; Li, C.; Han, S.; Sun, H.; Sun, M., *Trends Anal. Chem.* **2021**, *137*, 116208. **DOI:**10.1016/j.trac.2021.116208
11. Zheng, J.; Huang, S.; Tong, Y.; Wei, S.; Chen, G.; Huang, S.; Ouyang, G., *Anal. Chim. Acta* **2020**, *1137*, 28–36. **DOI:**10.1016/j.aca.2020.08.047
12. Cubillos, G. I.; Mendoza, M. E.; Alfonso, J. E.; Blanco, G.; Bethencourt, M., *Mater. Charact.* **2017**, *131*, 450–458. **DOI:**10.1016/j.matchar.2017.07.035
13. Lobe, S.; Bauer, A.; Uhlenbruck, S.; Fattakhova-Rohlfing, D., *Advanced Science* **2021**, *8* (11), 2002044. **DOI:**10.1002/advs.202002044
14. Xiang, Q.; Zhang, D.; Qin, J., *Mater. Lett.* **2016**, *176*, 127–130. **DOI:**10.1016/j.matlet.2016.04.105
15. Boccaccini, A. R.; Cho, J.; Roether, J. A.; Thomas, B. J. C.; Jane Minay, E.; Shaffer, M. S. P., *Carbon* **2006**, *44* (15), 3149–3160. **DOI:**10.1016/j.carbon.2006.06.021
16. Bagheri, H., Javanmardi, H., Abbasi, A., Banihashemi, S., *J. Chromatogr. A* **2016**, *1431*, 27–35. **DOI:**10.1016/j.chroma.2015.12.077
17. Ashour, R. M., Samouhos, M., Polido Legaria, E., Svärd, M.,

Högblom, J., Forsberg, K., Palmlöf, M., Kessler, V. G., Seisenbaeva, G. A., Rasmuson, Å. C., *ACS Sustain. Chem. Eng.* **2018**, *6* (5), 6889–6900. **DOI:**10.1021/acssuschemeng.8b00725
18. Das, D., Choudhury, P., Bortahkur, L., Gogoi, B., Buragohain, A. K., Dolui, S. K., *RSC Adv* **2015**, *5* (3), 2360–2367. **DOI:**10.1039/C4RA14444A
19. Rezaei, M., Tarvirdi-zadeh, R., *Int. J. New Chem.* **2019**, *6* (2), 76–86
20. Venkatesan, M. I., Northrup, T., Phillips, C. R., *J. Chromatogr. A* 2002, *942* (1), 223–230. **DOI:**10.1016/S0021-9673(01)01400-5
21. Hartmann, P. C., Quinn, J. G., King, J. W., Tsutsumi, S., Takada, H., *Environ. Sci. Technol.* **2000**, *34* (5), 900–906 **DOI:**10.1021/es990798q
22. Lu, J., Ye, F., Huang, X., Wei, L., Yao, D., Li, S., Ouyang, M., Lai, H., *J. Sep. Sci.* **2017**, *40* (5), 1133–1141. **DOI:**10.1002/jssc.201601144
23. Martins, C. C., Cabral, A. C., Barbosa-Cintra, S. C. T., Dauner, A. L. L., Souza, F. M., *Environ. Pollut.* **2014**, *188*, 71–80. **DOI:**10.1016/j.envpol.2014.01.022
24. Chen, B., Wang, S., Zhang, Q., Huang, Y., *Analyst* 2012, *137* (5), 1232–1240. **DOI:**10.1039/c2an16030g
25. Dalvand, K., Ghiasvand, A., *Anal. Chim. Acta* **2019**, *1083*, 119–129. **DOI:**10.1016/j.aca.2019.07.063
26. Zhang, G., Kataphinan, W., Teye-Mensah, R., Katta, P., Khatri, L., Evans, E. A., Chase, G. G., Ramsier, R. D., Reneker, D. H., *Mater. Sci. Eng. B* **2005**, *116* (3), 353–358. **DOI:**10.1016/j.mseb.2004.05.050
27. Naccarato, A., Tassone, A., Moretti, S., Elliani, R., Sprovieri, F., Pirrone, N., Tagarelli, A., *Talanta* **2018,** *189*, 657–665. **DOI:**10.1016/j.talanta.2018.07.077
28. Osooli, P., Yamini, Y., Tabibpour, M., Moosavi, N. S., *Microchim. Acta.* **2023**, *190* (12), 464. **DOI:**10.1007/s00604-023-06045-x
29. He, X.-M., Zhu, G.-T., Zheng, H.-B., Xu, S.-N., Yuan, B.-F., Feng, Y.-Q., *Talanta* **2015**, *140*, 29–35. **DOI:**10.1016/j.talanta.2015.03.006
30. Kim, M., Cho, S., Song, J., Son, S., Jang, J., *ACS Appl. Mat. Interfaces* **2012**, *4* (9), 4603–4609. **DOI:**10.1021/am300979s
31. Khalili, M., Dadfarnia, S., Haji Shabani, A. M., *J. Iran. Chem. Soc.* **2023**, *20* (7), 1719–1728. **DOI:**10.1007/s13738-023-02791-0
32. Sambyal, P., Ruhi, G., Dhawan, S. K., Bisht, B. M. S., Gairola, S. P., *Prog. Org. Coat.* **2018**, *119*, 203–213. **DOI:**10.1016/j.porgcoat.2018.02.014
33. Li, X., Dai, N., Wang, G., Song, X., *J.Appl. Polym. Sci.* **2008**, *107* (1), 403–408. **DOI:**10.1002/app.27153
34. Bezerra, M. A., Santelli, R. E., Oliveira, E. P., Villar, L. S., Escaleira, L. A., *Talanta* **2008**, *76* (5), 965–977. **DOI:**10.1016/j.talanta.2008.05.019
35. Ferreira, S. L. C., Bruns, R. E., Ferreira, H. S., Matos, G. D., David, J. M., Brandão, G. C., da Silva, E. G. P., Portugal, L. A., dos Reis, P. S., Souza, A. S., dos Santos, W. N. L., *Anal. Chim. Acta* **2007**, *597* (2), 179–186. **DOI:**10.1016/j.aca.2007.07.011
36. Alzaga, R., Peña, A., Ortiz, L., Marıa Bayona, J., *J. Chromatogr. A* **2003**, *999* (1), 51–60. **DOI:**10.1016/S0021-9673(03)00493-X
37. Darabi, J., Ghiasvand, A., Haddad, P. R., *Talanta* **2021**, *233*, 122583. **DOI:**10.1016/j.talanta.2021.122583
38. Hirayama, Y., Ikegami, H., Machida, M., Tatsumoto, H., *J. Health Sci.* **2006**, *52* (3), 228-236. **DOI:**10.1248/jhs.52.228
39. Čmelík, J., Brovdyová, T., Trögl, J., Neruda, M., Kadlečík, M., Pacina, J., Popelka, J., Sirotkin, A. S., *Water* **2019**, *11* (3), 481. **DOI:**10.3390/w11030481
40. Matuszewski, B. K., Constanzer, M. L., Chavez-Eng, C. M., *Anal. Chem.* **2003**, *75* (13) 3019–3030. **DOI:**10.1021/ac020361s

Povzetek

S kombinacijo elektronavitja in *in-situ* polimerizacije smo sintetizirali organsko-anorganski polianilin-SiO_2 (PANI/SiO_2) nanokompozit. Taka sintezna strategija je učinkovito minimizirala agregacijo PANI med polimerizacijo, kar je omogočilo višji izkoristek in izboljšano strukturno uniformnost. Izkoristili smo te izboljšane lastnosti in nanokompozit z elektrodepozicijo nanesli na žico iz nerjavnega jekla ter ga uporabili kot učinkovit sorbent za ekstrakcijo linearnih alkilbenzenov (LAB) z mikroekstrakcijo na trdno fazo iz nadprostora (HS-SPME), ki ji je sledila analiza s plinsko kromatografijo s plamensko-ionizacijsko detekcijo (GC-FID). Strukturo in morfologijo sintetiziranega sorbenta smo okarakterizirali s tehnikama vrstične elektronske mikroskopije (SEM) in infrardeče spektorskopije s Fourierjevo transformacijo (FT-IR). Za izbiro pomembnih eksperimentalnih parametrov smo uporabili metodologijo odzivne površine (RSM) s centralnim kompozitnim dizajnom (CCD). Pri optimalnih pogojih je bilo linearno dinamično območje (LDR) 0,05–12 ng mL^{-1} za Φ-C11 (undecilbenzen) in Φ-C13 (tridecilbenzen) ter 0,02–12 ng mL^{-1} za Φ-C12 (dodecilbenzen) in Φ-C14 (tetradecilbenzen) z regresijskimi koeficienti nad 0,99. Meje zaznave (LOD) so bile 0,007–0,015 ng mL^{-1}. Razvito HS-SPME-GC-FID metodo smo uspešno uporabili za ekstrakcijo in določitev LAB v vzorcih vode in odpadne vode.